arXiv:1403.3087v1 [astro-ph.SR] 12 Mar 2014

Spectroscopic analysis of cool giants and supergiants

Maria Bergemann, Rolf-Peter Kudritzki, and Ben Davies

Abstract Cool red giants and supergiants are among the most complex and fascinating stars in the Universe. They are bright and large, and thus can be observed to enormous distances allowing us to study the properties of their host galaxies, such as dynamics and chemical abundances. This review lecture addresses various problems related to observations and modelling spectra of red giants and supergiants.

1 Introduction

Cool evolved stars are perhaps the most enigmatic cosmic objects with luminosities spanning several orders of magnitude. The stars are at the end stages of stellar evolution (Fig. 1) occupying the coolest vertical strip on the Herzsprung-Russell diagram, the Hayashi limit for fully convective stars.

Low- and intermediate-mass stars evolve to the red giant branch (RGB) and asymptotic giant branch (AGB) after having spent most of their lifetime on the main sequence. These stars are cool and luminous, with effective temperatures $T_{\rm eff}$ between 2000 and 5500 K and luminosities L between 10 and 10^4 $L_{\odot}$. The stars have

M. Bergemann
Institute of Astronomy, University of Cambridge, CB3 0HA, Madingley Road, UK
e-mail: mbergema@ast.cam.ac.uk

Rolf-Peter Kudritzki
Institute for Astronomy, University of Hawaii, 2680 Woodlawn Drive, Honolulu, HI 96822, US;
Ludwig Maximilian University of Munich, Scheiner str. 1, 81679, Germany
e-mail: kud@ifa.hawaii.edu

Ben Davies
Astrophysics Research institute, Liverpool John Moores University, IC2, Liverpool Science Park,
146 Brownlow Hill, Liverpool L3 5RF, UK
e-mail: B.Davies@ljmu.ac.uk

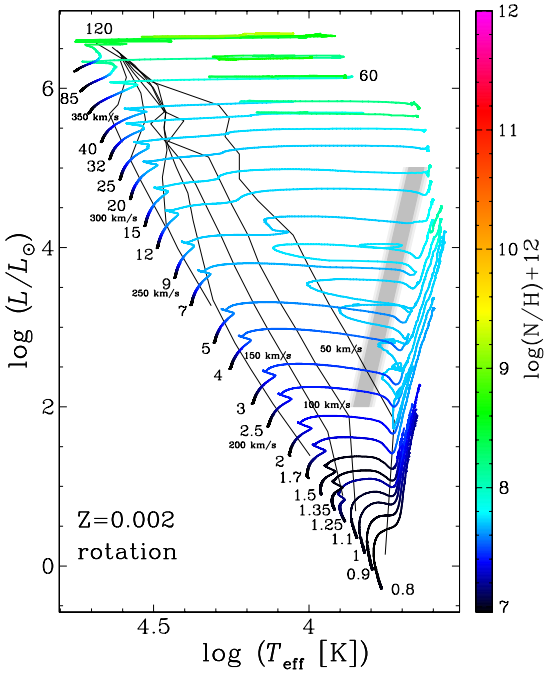

Fig. 1 Stellar tracks including the effect of rotation for stellar models with initial mass of 0.8 to 120 $M_{\odot}$ (Georgy et al, 2013). Cool giants and red supergiants occupy the stripe extending vertically from $1 < \log(L/L_{\odot}) < 6$.

a wide range of ages, from 1 to $>$ 10 Gyr, and thus trace chemical composition of interstellar matter in galaxies now and in the past.

High-mass stars are those with masses from 10 to 60 $M_{\odot}$; they evolve and explode quickly. Red supergiants (RSG) are young, typically $<$ 50 Myr, yet extremely bright with L from 10^4 to $10^6 L_{\odot}$.

Nucleosynthesis taking place in the interior of a star has as a consequence that, as evolution proceeds, stellar atmosphere acquires abundance patterns that strongly differ from the chemical composition of the natal cloud in which the star was born. This is referred to as self-pollution: dredge-up episodes bring material from the interior to the surface. Thus the stellar atmosphere becomes enriched or depleted in different chemical elements, e.g., He, C and N, and s-process elements (e.g. Lambert, 1992; Vassiliadis and Wood, 1993; Herwig, 2005). These abundance peculiarities are extreme on the AGB phase. The newly synthesised elements are returned into the ISM, as stars lose mass through winds. Giant stars are thus the primary producers of chemical elements, and much can be learned about stellar evolution from the analysis of abundance ratios as a function of the evolutionary stage of a star.

Giant stars serve as a primary gauge of cosmic abundances. They are the key targets in studies of Galactic chemical evolution and stellar archeology. Ongoing observational programmes search for very- and ultra-metal poor (UMP) stars in the Galactic halo and in the bulge (Beers and Christlieb, 2005); many of such objects are old red giants. Some large-scale stellar surveys, such as APOGEE (Apache Point Galactic Experiment from Sloan Digital Sky Survey) focus entirely on RGB stars,

for their intrinsic brightness allows to probe very large range of distances in the Galaxy. Individual giant stars can be observed with modern telescopes in the nearby galaxies of the Local Group (e.g. Guhathakurta et al, 2006; Kirby et al, 2010). Moreover, RGB and AGB stars dominate the integrated light of spatially unresolved systems, such as extra-Galactic globular clusters, dSph, and elliptical galaxies, thus allowing us to determine chemical composition of stellar populations from their composite spectra.

The atmospheres of giant stars are not fully in hydrostatic and thermodynamic equilibrium. Theory can explain observations only if very complex physical phenomena are included in the models: outflows, shocks, winds, pulsations, indicating that we are dealing with stars far more complex than the Sun. Violent convective motions penetrate their atmospheres and influence the physical state of matter. The extremely low densities of giant photospheres are to be blamed for the fact that matter and radiation are not in equilibrium.

All these phenomena will be briefly reviewed below (for a status update see also the review by Ryde, 2010). First, we recap the most recent results from imaging and spectroscopy of cool stars (Sec. 2), which convincingly show that the stars are more sophisticated compared to their evolutionary predecessors, un-evolved main-sequence stars, and give a glimpse to their complex physics. Sec. 3 describes the methods used for stellar parameter analysis. In Sec. 4, we review the key results of state-of-the-art modelling of cool giant spectra[1].

2 Observations

With the recent developments in astronomical instrumentation, in particular adaptive optics, it has become possible to obtain unique observations of giants in their native spectral range, infra-red (IR)[2].

Diffraction-limited imaging observations of giants and supergiants can be done with ground-based interferometric telescopes, such as VLT/NACO (Kervella et al, 2009). Surface inhomogeneities on RSGs were detected in the JHK bands. Betelgeuse, our closest red supergiant with a radius $R \sim 800 R_{\odot}$, appears to have a complex circumstellar envelope with an outflow, or plume, extending to enormous distances of several stellar radii (Fig. 2). A combined analysis of different photometric bands suggests the presence of a very cool layer on top of the Betelgeuse's photosphere, perhaps made of CN or water molecules (Kervella et al, 2009), and dusty envelopes, which produce flux excess in the far-IR stellar spectral energy distributions (Tsuji, 2000). Interferometric long-baseline observations in optical filters (Quirrenbach et al, 1993), discovered another interesting effect: the star imaged in different filters, e.g. TiO 712 nm vs continuum at 754 nm, has a different size! The

[1] A more detailed discussion of model atmospheres and synthetic spectra for giants are given in the review lecture on 3D NLTE spectroscopy.

[2] Very cool stars, such as RGB and RSG, emit the most light in the IR.

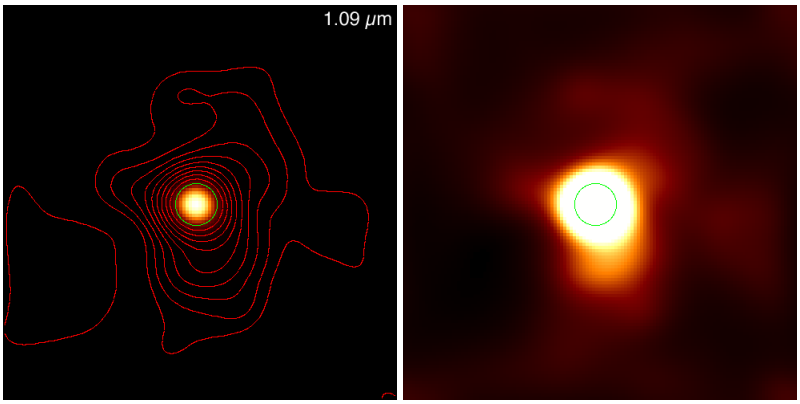

Fig. 2 Interferometric observations of Betelgeuse taken with VLT/NACO at 1.09μm (Kervella et al, 2009). The left image has a linear colour scale; the contours indicate different flux levels in increasing powers of 2. The right plot corresponds to a square-root colour scale and it also shows the photospheric radius of the star at 43.7 mas (green circle).

difference in diameter for the coolest M-type giants and supergiants is nearly 10 %, which suggests huge extension of their atmospheres.

Other interesting results about atmospheric structure and dynamics of cool stars were delivered by space missions, such as the Herschel Space Observatory (Teyssier et al, 2012, HSO, e.g.). Fig. 3 shows the image of Betelgeuse made by superposition of images taken at 70 to 160 μm (Decin et al, 2012). The image reveals a dusty envelope and multiple arc-like structures caused by the interaction of stellar wind and interstellar matter, so-called bow shocks. The morphology of these structures can be explained by sophisticated 3D time-dependent hydrodynamical simulations of the stellar envelopes.

Spectroscopic observations reveal complexities of a different type. Red giants and supergiants are very cool stars, with effective temperatures from $\sim$ 3000 to 5000 K. In these conditions, various molecules very efficiently absorb radiation. Thus, the spectra are severely distorted by molecular bands, such as CN, NH, H_2O, and particularly TiO (Allard et al, 2000), which absorbs most of the radiation in the optical window (Fig. 4 top panel). Although molecules are ubiquitous and are sensitive probes of atmospheric physics, their modelling is very difficult (Sec 4) and complex 3D radiative hydrodynamics calculations are needed (Uitenbroek and Criscuoli, 2011).

Very high-resolution observations of cool giants (e.g. Dravins, 1990; Gray et al, 2008; Ramírez et al, 2010; Gray, 2012) show that the spectral lines are not symmetric. The reversed-*C* shapes of the line profiles indicate large convection cells at the surface of stars.

The IR part of giant spectra is much less contaminated by molecular absorption that significantly simplifies the problem of spectral analysis. Targeting the near-IR region also has the benefit that the stellar flux is less extinguished by interstellar absorption, allowing studies deep into the galaxy. For example, cool giants and su-

pergiants have been used to study the abundances in the Galactic Centre (Carr et al, 2000; Cunha et al, 2007; Davies et al, 2009b), the Scutum Arm tangent and the end of the Galactic Bar (Davies et al, 2009a), and the Galactic Bulge (Rich et al, 2007).

Thus in terms of science, spectroscopy of RGB, AGB, and RSG stars has a great potential in the IR.

3 Stellar parameters

The basic parameters of cool stars can be estimated by different methods. Here, we focus on the spectroscopic techniques that have been developed to determine effective temperature $T_{\rm eff}$, surface gravity $\log g$, and metallicity $[{\rm Fe}/{\rm H}]$ of a star.

The perhaps most stable and simple method to estimate stellar parameters is the method of excitation-ionization balance for a pair of chemical species, such as Fe I and Fe II. The simplicity comes mainly from the application of the curve-of-growth technique (Gray, 2008). First, one computes the abundance from the measured line equivalent width. The $T_{\rm eff}$ is then set by minimising the magnitude of the slope of the relationship between the abundance of iron from Fe I lines and the excitation potential of each line. The surface gravity is then estimated by minimising the difference between the abundance of iron measured from Fe I and Fe II lines. Iterations are

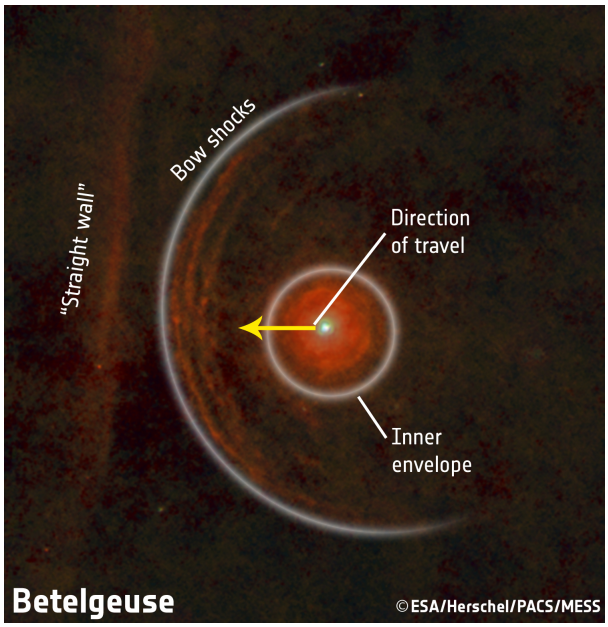

Fig. 3 Herschel image of Betelgeuse (Decin et al, 2012). The image shows the morphology of the stars's environment (see text).

needed to have the above criteria satisfied. The method offers several advantages: efficiency, fast convergence, and easy implementation. The downside is the need for a statistically significant sample of clean unblended lines; moreover, the method is very sensitive to the physics of the models. Recent studies showed that standard 1D hydrostatic model atmospheres and LTE line formation fail for giant stars, producing unphysically low estimates of temperature, surface gravity, and metallicity (e.g. Bergemann et al, 2012b; Ruchti et al, 2013).

For cooler stars, such as RSG, the excitation-ionization balance method is not useful. First, their optical spectra are too blended to allow a meaningful estimate of a line equivalent width. Adjacent spectral lines fuse with one another, and it is not possible to separate their individual profiles. Second, most of the lines from singly-ionized element vanish, and there is no constraint on the ionization balance. The method of global spectrum synthesis (Fig. 5), which relies on all spectral lines present in the observed spectrum, is much more suitable for the analysis of RSGs. Each parameter affects the relative strengths of the lines in subtly different ways, meaning that the parameters may be determined via a χ^2 minimisation search within a precomputed grid of model spectra (see Gazak et al. 2014, submitted).

The principal diagnostics of effective temperatures for RSGs have been the strengths of the optical TiO bands which define the spectral classification sequence. These features were modelled by Levesque et al (2005, 2006) using the MARCS model atmospheres in order to determine the temperature scale for such stars. However, it has since been shown that, as a consequence of deviations from hydrostatic equilibrium in RSG atmospheres, the 1D hydrostatic models underpredict the strengths of the TiO bands (Fig. 6). This leads to effective temperatures which are too low (Davies et al, 2013). Spectra computed with 3D hydrodynamical models (Fig. 7, see also Sec. 4.1) tend to have deeper TiO absorption bands and brighter fluxes at the minimum of opacity, 1.6μm, compared to 1D hydrostatic models thus alleviating the problem, at least in part.

Red giants and supergiants are very useful as metallicity indicators. Their spectra are rich in metallic lines, allowing for abundances to be determined for a range of elements. Such work typically targets the near-IR, which coincides with the flux peak of the stars, and which avoids the regions of the spectrum dominated by problematic TiO bands. More recently, this work is being adapted so that metallicities may be retrieved at lower spectral resolutions. This is done by isolating a region in the *J*-band (Fig. 5) which is relatively free of the molecular lines that plague the spectra of these stars, alleviating the problem of line-blending. This means that RSGs may be studied at distances of several Mpc, making them excellent probes of their host galaxies' abundances Davies et al (2010). The atomic lines of Fe, Ti, Si and Mg present in this region provide sufficient information to solve for the primary free parameters in model atmospheres, i.e. effective temperature, gravity, microturbulence and metallicity.

4 Physics of giant atmospheres

Here we review those aspects of the physics of giants and RGSs, which can be presently addressed with theoretical models of atmospheres and spectral line formation. These aspects include:

- Molecular line opacities
- Deviations from hydrostatic equilibrium
- Deviations from local thermodynamic equilibrium
- Chromospheres, MOLspheres, winds, mass loss

For some of these aspects, such as MOLspheres[3] and chromospheres (see below), the models are semi-empirical, in a sense that they are tuned to reproduce observations.

NLTE and 3D hydrodynamical calculations can be performed based on *ab initio* physical considerations.

4.1 Molecular line opacities

Until recently, one of the main limitations of spectroscopic models for giants was the absence of accurate data for molecular line transitions. Complete TiO linelists, which include tens of millions of transitions, have been published only recently (Plez, 1998). However, other diatomic molecules have a significant contribution in giant spectra, including CN, CO, MgH, VO (de Laverny et al, 2012). The major challenge is to include all these atomic data in spectral synthesis codes and stellar atmosphere models to correctly recover their temperature and pressure structures and predict the emergent spectra. So far, only simplified 1D LTE hydrostatic models, like MARCS (Gustafsson et al, 2008) or PHOENIX (Hauschildt et al, 1997), which include accurate opacity sampling (OS) schemes, have been able to cope with the bulky linelists. Such models are used to model RSG and RGB spectra at present.

4.2 3D hydrodynamics and giant convective cells

Recently, it became possible to compute 2D and 3D radiative hydrodynamics (3D RHD) models of stellar convection (e.g. Stein and Nordlund 1998, Freytag et al 2002, Chiavassa et al 2011). Depending on the properties of a star, e.g. a smaller giant or a larger supergiant, the codes may work in two diametrally different modes. The first local setup is known as *box-in-a-star* and it is usually applied to modelling solar-like stars (e.g. Freytag et al, 2002). The second, global *star-in-a-box*

[3] MOLsphere is a term used for a warm optically-thick water envelope around cool stars, which has been proposed in some studies to explain the IR observations (Tsuji, 2001).

setup is applied to model very extended, variable and stochastically pulsating stars. These are characteristics of red supergiants. The difference is essentially that in the local setup, the equations of compressible hydrodynamics and non-local radiation transport are solved only in a small box on a surface of a star. In contrast, in the *star-in-a-box* regime, the simulation box includes the whole star.

The 3D RHD[4] models are much more successful than classical 1D hydrostatic models in reproducing a wealth of observational information, including the line shapes and bisectors, center-to-limb variation, and brightness contrast (Asplund, 2005). However, such models are exceptionally sophisticated and can not be computed for a large range of stellar parameters due to prohibitively long computation times. At present, the use of 3D RHD models is restricted to the analysis of individual stars, such as the bright metal-poor giant HD 122563 (Collet et al, 2009) and the red supergiant Betelgeuse (Chiavassa et al, 2010). The 3D RHD models are also used to explore the validity range of simpler 1D hydrostatic model atmospheres (e.g. Collet et al, 2007).

Fig. 8 shows a snapshot from a star-in-a-box simulation of convection on Betelgeuse, as computed with the CO5BOLD code (Chiavassa et al, 2011). The emergent intensity is shown at the wavelength of 500 nm. Huge giant convection cells predicted by the model are consistent with imaging observations of the star from space, e.g from the Hubble Space Telescope (Gilliland and Dupree, 1996).

4.3 NLTE

Another major complication in the analysis of spectra of cool giants is to include departures from Local Thermodynamic Equilibrium (LTE). As a consequence of very low surface densities, $-0.5 < \log g < 3$, collisions between particles are too weak to establish local equilibrium in a stellar atmosphere. Each parcel of the gas is influenced by photons originating elsewhere. This is what we call - *non-local radiation field*, and thus non-local thermodynamic equilibrium. Research in NLTE physics of cool giant and supergiant atmospheres is still at its infancy, however, it is clear already now that spectral lines of different atoms and molecules do not form under LTE conditions.

Bergemann et al (2012b,a, 2013) proved from *ab initio* statistical equilibrium calculations, that ions such as Fe I, Ti I, Si I, Cr I, Ti I, are very sensitive to strong photo-ionising radiation fields. In this case, the effect of NLTE is to reduce the number densities of atoms in a minority ionisation stage, thus for a given abundance the line equivalent width is smaller than that given by LTE. This effect is larger in metal-poor stars. At solar metallicity, the opposite behaviour is encountered sometimes. For example, the IR transitions of Si I and Ti I show *negative* NLTE effects such that the LTE abundance is higher than the NLTE one (Fig. 9). According to recent studies, the LTE and NLTE abundances may differ by an order of magnitude,

[4] See the review lecture on 3D NLTE spectroscopy in the book.

from -0.5 to $+1.0$ dex, depending on the element and ionisation stage, intrinsic line parameters (wavelength, level excitation potential), and stellar parameters.

The NLTE analysis of molecular spectral lines is an unexplored territory. New studies show the effect of NLTE in is to cause stronger molecular absorption bands that leads to extra cooling in the outer atmospheric layers (Lambert et al, 2013).

Detailed theoretical and observational studies are necessary to understand how NLTE influences the estimates of stellar parameters and abundances from giant spectra.

4.4 Chromospheres, MOLspheres, winds, and mass loss

Fig. 10 shows the late-type stars in the H-R diagram (Ayres, 2010). The illustration is similar to the Linsky and Haisch (1979) diagram of *solar* and *non-solar* type stars; the former with chromospheres, transition regions, and coronae, and the latter with chromospheres only. It is thought that the absence of a corona is a consequence of strong winds (see also Dehaes et al, 2011).

Chromospheres are easy to detect through observations. For instance, high-quality spectroscopic observations of RGB tip stars in globular clusters produced compelling evidence for chromospheric activity, based on the emission wings of H_α line at 656.3 nm (Meszaros et al, 2008). Accoridng to models, the wings form in the chromosphere[5], although they are also affected by stellar pulsations. Other diagnostic features sensitive to activity are the UV Ca H and K lines at 395 nm and the Mg II resonance lines at at 280 nm (e.g. Leenaarts et al, 2013). These strong lines develop chromospheric emission in the innermost cores. Since stellar rotation, and thus chromospheric activity, declines with the age of a star, the strength of the line core emission is a useful measure of stellar ages (Soderblom et al, 1991). Strong correlation was also discovered between the strengths of Mg II resonance lines and TiO molecular bands (Steiman-Cameron et al, 1985).

The inability to fit some features in the IR spectra of cool giants with 1D hydrostatic LTE models gave rise to extensions of the classical models. Such extended models, for example, include MOLsphere, a very cool molecular layer above the photosphere (Tsuji, 2001, 2008). The models assume a very low temperature of $1000-2000$ K and the column density of molecules is adjusted to fit the observed spectra. It is unclear whether the appeal to such ad-hoc extensions is justified given the major uncertainties in the analysis of molecular spectral lines caused by the limitations of 1D hydrostatic models with LTE.

Red giants and supergiants lose mass through low-speed winds of few tens of km/s. The rate of mass loss can be very high, for AGB stars up to $10^{-5}M_\odot$/year and for RSGs up to $10^{-4}M_\odot$/year (De Beck et al, 2010). In- and out-flow motions are 'seen' in the high-resolution spectra of giants: the most pronounced features are shifts and asymmetries of strong line cores, like H_α. Mass outflows are responsible

[5] Interestingly, only stars with $log(L/L_\odot) \geq 2.4$ show emission wings.

for the circumstellar shells that cause IR emission in the stellar spectra. Some insight into the mass loss phenomenon can also be gained from interferometry. It has been suggested that RSG winds contribute to larger radii at 712 nm as measured by interferometric techniques.

Models of oxygen-rich stars with effective temperatures below 3000 K must include dust formation (Ferguson et al, 2001). The effect of the latter is two-fold: dust condensation warms up the atmosphere and decreases the abundance of elements locked up in the gas phase. Different elements, such as Ti, Zr, and Al, condense into dust grains. For an observer, the most relevant is the change in the number density of TiO, which can be detected in the spectra. The impact of more sophisticated models on the abundance analysis and stellar parameter determinations remains to be quantified.

5 Conclusions

To conclude, modelling spectra of cool giants and supergiants is, doubtlessly, a very challenging problem. Different physical phenomena must be included in the atmosphere and line formation models to allow for an accurate determination of surface parameters: molecular line opacities, deviations from 1D hydrostatic equilibrium and from local thermodynamic equilibrium, chromospheres, winds, and mass loss. We have attained the necessary minimum level of complexity to address the simpler problems, like the determination of metallicity and bolometric flux. However, more detailed investigations, like the analysis of TiO or CO molecular bands and the interpretation of strong lines like H_α, Ca H & K, Mg II, which contain the essential physics, shall await for more complex models including the above-mentioned effects. In the view of the enormous perspectives offered by observing giants and RSGs throughout the Milky Way and in other galaxies, the need for more physically-realistic models is well-justified.

Acknowledgements Figures from the following papers have been reproduced with permission from the authors and from the publishers (c) ESO: Chiavassa et al. A &A, 535, A22, 2011; Decin et al. A&A, 548, A113, 2012; Georgy et al. A&A, 558, A103, 2013; Lancon & Wood, A&AS, 146, 217, 2000; Kervella et al., A&A, 504, 115, 2009. Figures from the following papers have been reproduced by permission of the AAS: Davies et al., ApJ, 767:3, 2013. This work was partly supported by the European Union FP7 programme through ERC grant number 320360.

References

Allard F, Hauschildt PH, Schwenke D (2000) TIO and H_2O Absorption Lines in Cool Stellar Atmospheres. ApJ540:1005–1015, DOI 10.1086/309366, astro-ph/0008465

Asplund M (2005) New Light on Stellar Abundance Analyses: Departures from LTE and Homogeneity. ARA&A43:481–530, DOI 10.1146/annurev.astro.42.053102.134001

Ayres T (2010) A stellar perspective on chromospheres. Mem. Soc. Astron. Italiana81:553

Beers TC, Christlieb N (2005) The Discovery and Analysis of Very Metal-Poor Stars in the Galaxy. ARA&A43:531–580, DOI 10.1146/annurev.astro.42.053102.134057

Bergemann M, Kudritzki RP, Plez B, Davies B, Lind K, Gazak Z (2012a) Red Supergiant Stars as Cosmic Abundance Probes: NLTE Effects in J-band Iron and Titanium Lines. ApJ751:156, DOI 10.1088/0004-637X/751/2/156, 1204.0511

Bergemann M, Lind K, Collet R, Magic Z, Asplund M (2012b) Non-LTE line formation of Fe in late-type stars - I. Standard stars with 1D and ¡3D¿ model atmospheres. MNRAS427:27–49, DOI 10.1111/j.1365-2966.2012.21687.x, 1207.2455

Bergemann M, Kudritzki RP, Würl M, Plez B, Davies B, Gazak Z (2013) Red Supergiant Stars as Cosmic Abundance Probes. II. NLTE Effects in J-band Silicon Lines. ApJ764:115, DOI 10.1088/0004-637X/764/2/115, 1212.2649

Carr JS, Sellgren K, Balachandran SC (2000) The First Stellar Abundance Measurements in the Galactic Center: The M Supergiant IRS 7. ApJ530:307–322, DOI 10.1086/308340, astro-ph/9909037

Chiavassa A, Haubois X, Young JS, Plez B, Josselin E, Perrin G, Freytag B (2010) Radiative hydrodynamics simulations of red supergiant stars. II. Simulations of convection on Betelgeuse match interferometric observations. A&A515:A12, DOI 10.1051/0004-6361/200913907, 1003.1407

Chiavassa A, Freytag B, Masseron T, Plez B (2011) Radiative hydrodynamics simulations of red supergiant stars. IV. Gray versus non-gray opacities. A&A535:A22, DOI 10.1051/0004-6361/201117463, 1109.3619

Collet R, Asplund M, Trampedach R (2007) Three-dimensional hydrodynamical simulations of surface convection in red giant stars. Impact on spectral line formation and abundance analysis. A&A469:687–706, DOI 10.1051/0004-6361:20066321, astro-ph/0703652

Collet R, Nordlund Å, Asplund M, Hayek W, Trampedach R (2009) Abundance analysis of the halo giant HD 122563 with three-dimensional model stellar atmospheres. Memorie della Societa Astronomica Italiana 80:719, 0909.0690

Cunha K, Sellgren K, Smith VV, Ramirez SV, Blum RD, Terndrup DM (2007) Chemical Abundances of Luminous Cool Stars in the Galactic Center from High-Resolution Infrared Spectroscopy. ApJ669:1011–1023, DOI 10.1086/521813, 0707.2610

Davies B, Origlia L, Kudritzki RP, Figer DF, Rich RM, Najarro F (2009a) The Chemical Abundances in the Galactic Center from the Atmospheres of Red Supergiants. ApJ694:46–55, DOI 10.1088/0004-637X/694/1/46, 0811.3179

Davies B, Origlia L, Kudritzki RP, Figer DF, Rich RM, Najarro F, Negueruela I, Clark JS (2009b) Chemical Abundance Patterns in the Inner Galaxy: The Scutum

Red Supergiant Clusters. ApJ696:2014–2025, DOI 10.1088/0004-637X/696/2/2014, 0902.2378

Davies B, Kudritzki RP, Figer DF (2010) The potential of red supergiants as extragalactic abundance probes at low spectral resolution. MNRAS407:1203–1211, DOI 10.1111/j.1365-2966.2010.16965.x, 1005.1008

Davies B, Kudritzki RP, Plez B, Trager S, Lançon A, Gazak Z, Bergemann M, Evans C, Chiavassa A (2013) The Temperatures of Red Supergiants. ApJ767:3, DOI 10.1088/0004-637X/767/1/3, 1302.2674

De Beck E, Decin L, de Koter A, Justtanont K, Verhoelst T, Kemper F, Menten KM (2010) Probing the mass-loss history of AGB and red supergiant stars from CO rotational line profiles. II. CO line survey of evolved stars: derivation of mass-loss rate formulae. A&A523:A18, DOI 10.1051/0004-6361/200913771, 1008.1083

de Laverny P, Recio-Blanco A, Worley CC, Plez B (2012) The AMBRE project: A new synthetic grid of high-resolution FGKM stellar spectra. A&A544:A126, DOI 10.1051/0004-6361/201219330, 1205.2270

Decin L, Cox NLJ, Royer P, Van Marle AJ, Vandenbussche B, Ladjal D, Kerschbaum F, Ottensamer R, Barlow MJ, Blommaert JADL, Gomez HL, Groenewegen MAT, Lim T, Swinyard BM, Waelkens C, Tielens AGGM (2012) The enigmatic nature of the circumstellar envelope and bow shock surrounding Betelgeuse as revealed by Herschel. I. Evidence of clumps, multiple arcs, and a linear bar-like structure. A&A548:A113, DOI 10.1051/0004-6361/201219792, 1212.4870

Dehaes S, Bauwens E, Decin L, Eriksson K, Raskin G, Butler B, Dowell CD, Ali B, Blommaert JADL (2011) Structure of the outer layers of cool standard stars. A&A533:A107, DOI 10.1051/0004-6361/200912442

Dravins D (1990) Stellar granulation. VI - Four-component models and non-solar-type stars. A&A228:218–230

Ferguson JW, Alexander DR, Allard F, Hauschildt PH (2001) Grains in the Atmospheres of Red Giant Stars. ApJ557:798–801, DOI 10.1086/321680

Freytag B, Steffen M, Dorch B (2002) Spots on the surface of Betelgeuse – Results from new 3D stellar convection models. Astronomische Nachrichten 323:213–219, DOI 10.1002/1521-3994(200208)323:3/4⟨213::AID-ASNA213⟩3.0.CO;2-H

Georgy C, Ekström S, Eggenberger P, Meynet G, Haemmerlé L, Maeder A, Granada A, Groh JH, Hirschi R, Mowlavi N, Yusof N, Charbonnel C, Decressin T, Barblan F (2013) Grids of stellar models with rotation. III. Models from 0.8 to 120 $M_\odot$ at a metallicity Z = 0.002. A&A558:A103, DOI 10.1051/0004-6361/201322178, 1308.2914

Gilliland RL, Dupree AK (1996) First Image of the Surface of a Star with the Hubble Space Telescope. ApJ463:L29, DOI 10.1086/310043

Gray DF (2008) The Observation and Analysis of Stellar Photospheres

Gray DF (2012) Granulation in the Photosphere of ζ Cygni. AJ143:112, DOI 10.1088/0004-6256/143/5/112

Gray DF, Carney BW, Yong D (2008) Asymmetries in the Spectral Lines of Evolved Halo Stars. AJ135:2033–2037, DOI 10.1088/0004-6256/135/6/2033

Guhathakurta P, Rich RM, Reitzel DB, Cooper MC, Gilbert KM, Majewski SR, Ostheimer JC, Geha MC, Johnston KV, Patterson RJ (2006) Dynamics and Stellar Content of the Giant Southern Stream in M31. I. Keck Spectroscopy of Red Giant Stars. AJ131:2497–2513, DOI 10.1086/499562, astro-ph/0406145

Gustafsson B, Edvardsson B, Eriksson K, Jørgensen UG, Nordlund Å, Plez B (2008) A grid of MARCS model atmospheres for late-type stars. I. Methods and general properties. A&A486:951–970, DOI 10.1051/0004-6361:200809724, 0805.0554

Hauschildt PH, Baron E, Allard F (1997) Parallel Implementation of the PHOENIX Generalized Stellar Atmosphere Program. ApJ483:390, DOI 10.1086/304233, astro-ph/9607087

Herwig F (2005) Evolution of Asymptotic Giant Branch Stars. ARA&A43:435–479, DOI 10.1146/annurev.astro.43.072103.150600

Kervella P, Verhoelst T, Ridgway ST, Perrin G, Lacour S, Cami J, Haubois X (2009) The close circumstellar environment of Betelgeuse. Adaptive optics spectro-imaging in the near-IR with VLT/NACO. A&A504:115–125, DOI 10.1051/0004-6361/200912521, 0907.1843

Kirby EN, Guhathakurta P, Simon JD, Geha MC, Rockosi CM, Sneden C, Cohen JG, Sohn ST, Majewski SR, Siegel M (2010) Multi-element Abundance Measurements from Medium-resolution Spectra. II. Catalog of Stars in Milky Way Dwarf Satellite Galaxies. ApJS191:352–375, DOI 10.1088/0067-0049/191/2/352, 1011.4516

Lambert DL (1992) Observational Effects of Nucleosynthesis in Evolved Stars. In: Edmunds MG, Terlevich R (eds) Elements and the Cosmos, p 92

Lambert J, Josselin E, Ryde N, Faure A (2013) NLTE water lines in Betelgeuse-like atmospheres. In: Kervella P, Le Bertre T, Perrin G (eds) EAS Publications Series, EAS Publications Series, vol 60, pp 111–119, DOI 10.1051/eas/1360012, 1304.4111

Lançon A, Wood PR (2000) A library of 0.5 to 2.5 mu m spectra of luminous cool stars. A&AS146:217–249, DOI 10.1051/aas:2000269

Leenaarts J, Pereira TMD, Carlsson M, Uitenbroek H, De Pontieu B (2013) The Formation of IRIS Diagnostics. II. The Formation of the Mg II H & K Lines in the Solar Atmosphere. ApJ772:90, DOI 10.1088/0004-637X/772/2/90, 1306.0671

Levesque EM, Massey P, Olsen KAG, Plez B, Josselin E, Maeder A, Meynet G (2005) The Effective Temperature Scale of Galactic Red Supergiants: Cool, but Not As Cool As We Thought. ApJ628:973–985, DOI 10.1086/430901, astro-ph/0504337

Levesque EM, Massey P, Olsen KAG, Plez B, Meynet G, Maeder A (2006) The Effective Temperatures and Physical Properties of Magellanic Cloud Red Supergiants: The Effects of Metallicity. ApJ645:1102–1117, DOI 10.1086/504417, astro-ph/0603596

Linsky JL, Haisch BM (1979) Outer atmospheres of cool stars. I - The sharp division into solar-type and non-solar-type stars. ApJ229:L27–L32, DOI 10.1086/182924

Meszaros S, Dupree AK, Szentgyorgyi A (2008) Mass Outflow and Chromospheric Activity of Red Giant Stars in Globular Clusters.I. M15. AJ135:1117–1135, DOI 10.1088/0004-6256/135/4/1117, 0801.0433

Plez B (1998) A new TiO line list. A&A337:495–500

Quirrenbach A, Hummel CA, Buscher DF, Armstrong JT, Mozurkewich D, Elias NM II (1993) The Asymmetric Envelope of gamma Cassiopeiae Observed with the MK III Optical Interferometer. ApJ416:L25, DOI 10.1086/187062

Ramírez I, Collet R, Lambert DL, Allende Prieto C, Asplund M (2010) Granulation Signatures in the Spectrum of the Very Metal-poor Red Giant HD 122563. ApJ725:L223–L227, DOI 10.1088/2041-8205/725/2/L223, 1011.4077

Rich RM, Origlia L, Valenti E (2007) The First Detailed Abundances for M Giants in the Inner Bulge from Infrared Spectroscopy. ApJ665:L119–L122, DOI 10.1086/521440, 0707.1855

Ruchti GR, Bergemann M, Serenelli A, Casagrande L, Lind K (2013) Unveiling systematic biases in the 1D LTE excitation-ionization balance of Fe for FGK stars: a novel approach to determination of stellar parameters. MNRAS429:126–134, DOI 10.1093/mnras/sts319, 1210.7998

Ryde N (2010) Prospects of stellar abundance studies from near-IR spectra observed with the E-ELT. Astronomische Nachrichten 331:433, DOI 10.1002/asna.200911345, 1002.3038

Soderblom DR, Duncan DK, Johnson DRH (1991) The chromospheric emission-age relation for stars of the lower main sequence and its implications for the star formation rate. ApJ375:722–739, DOI 10.1086/170238

Steiman-Cameron TY, Johnson HR, Honeycutt RK (1985) Chromospheric activity and TiO bands in M giants. ApJ291:L51–L54, DOI 10.1086/184457

Stein RF, Nordlund A (1998) Simulations of Solar Granulation. I. General Properties. ApJ499:914, DOI 10.1086/305678

Teyssier D, Quintana-Lacaci G, Marston AP, Bujarrabal V, Alcolea J, Cernicharo J, Decin L, Dominik C, Justtanont K, de Koter A, Melnick G, Menten KM, Neufeld DA, Olofsson H, Planesas P, Schmidt M, Soria-Ruiz R, Schöier FL, Szczerba R, Waters LBFM (2012) Herschel/HIFI observations of red supergiants and yellow hypergiants. I. Molecular inventory. A&A545:A99, DOI 10.1051/0004-6361/201219545, 1208.3143

Tsuji T (2000) Water on the Early M Supergiant Stars α Orionis and μ Cephei. ApJ538:801–807, DOI 10.1086/309185

Tsuji T (2001) Water in K and M giant stars unveiled by ISO. A&A376:L1–L4, DOI 10.1051/0004-6361:20011012, astro-ph/0109004

Tsuji T (2008) Cool luminous stars: the hybrid nature of their infrared spectra. Astronomy & Astrophysics 489(3):1271–1289

Uitenbroek H, Criscuoli S (2011) Why One-dimensional Models Fail in the Diagnosis of Average Spectra from Inhomogeneous Stellar Atmospheres. ApJ736:69, DOI 10.1088/0004-637X/736/1/69, 1101.2643

Vassiliadis E, Wood PR (1993) Evolution of low- and intermediate-mass stars to the end of the asymptotic giant branch with mass loss. ApJ413:641–657, DOI 10.1086/173033

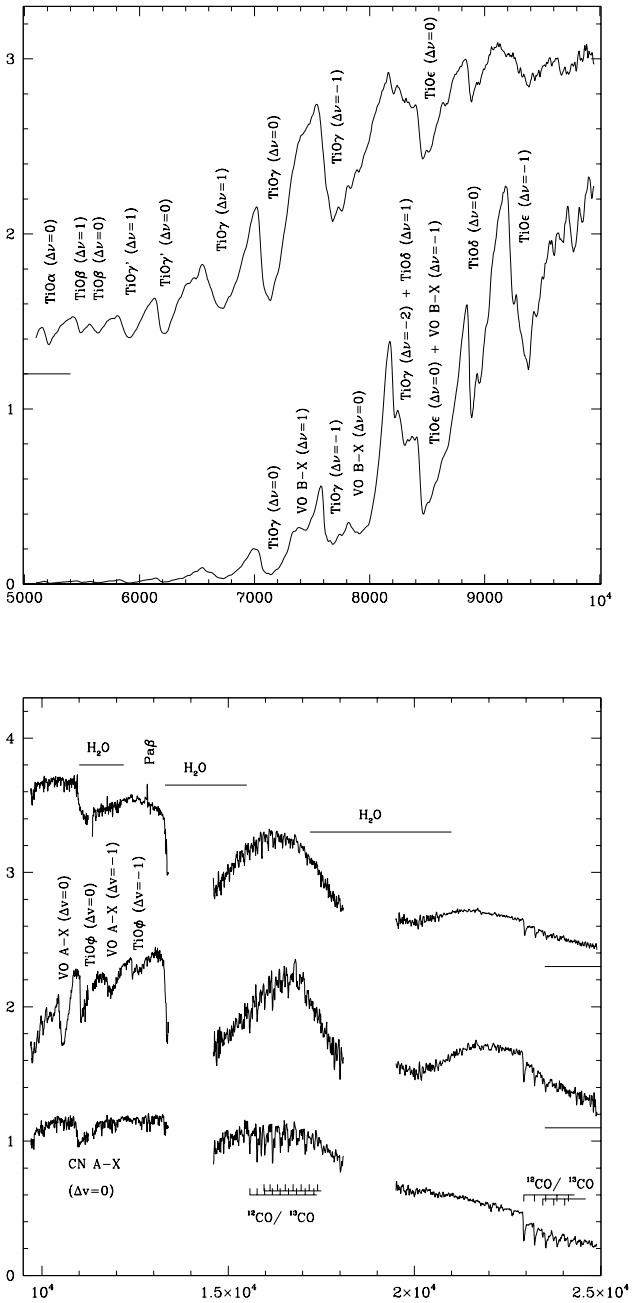

Fig. 4 Spectra of cool stars (Lançon and Wood, 2000). Top: a spectrum of a warm Mira star in the optical window below 1μm; the TiO bands are prominent. Bottom: the IR spectra of a warm Mira star, cool Mira star, and the red supergiant (top to bottom).

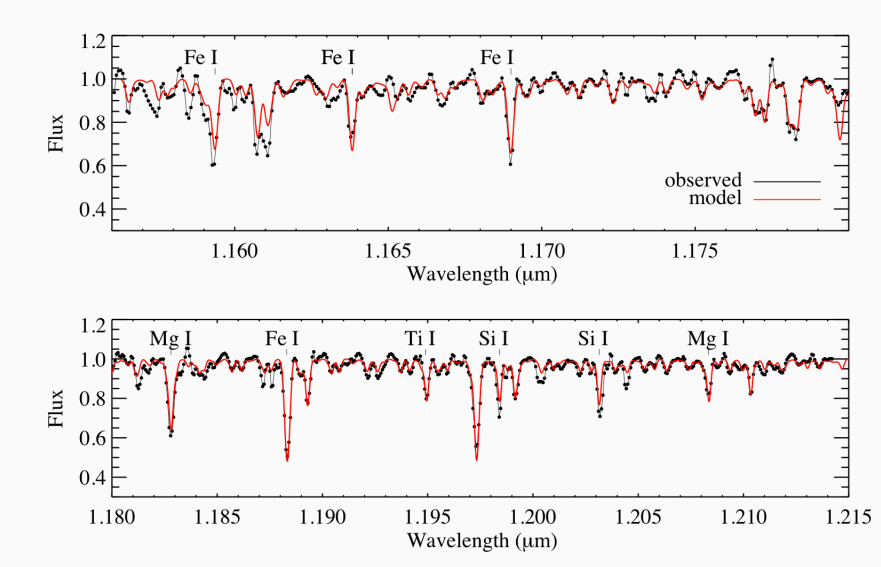

Fig. 5 Comparison of the observed (black) and theoretical NLTE (red) spectra for Betelgeuse.

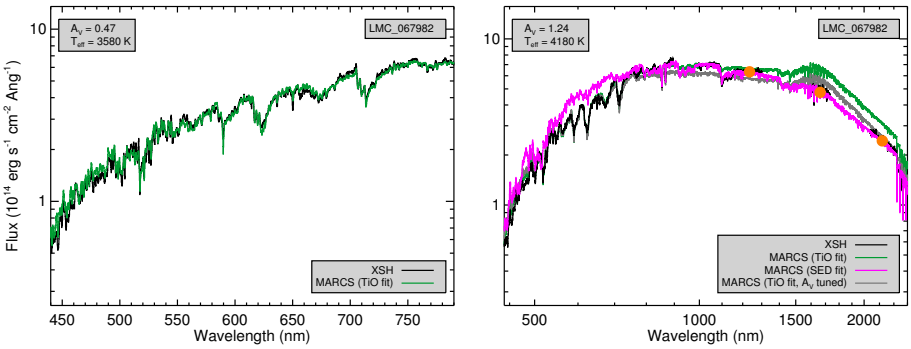

Fig. 6 A theoretical fit to the optical spectrum (left) and to the complete SED for a red supergiant in LMC (Davies et al. 2013). The observed spectrum from the X-Shooter instrument at VLT is shown with a black line. On the right plot, the magenta and green lines correspond to the MARCS 1D LTE theoretical spectra computed with different $T_{\rm eff}$. The orange symbols indicate spectro-photometric measurements for the star.

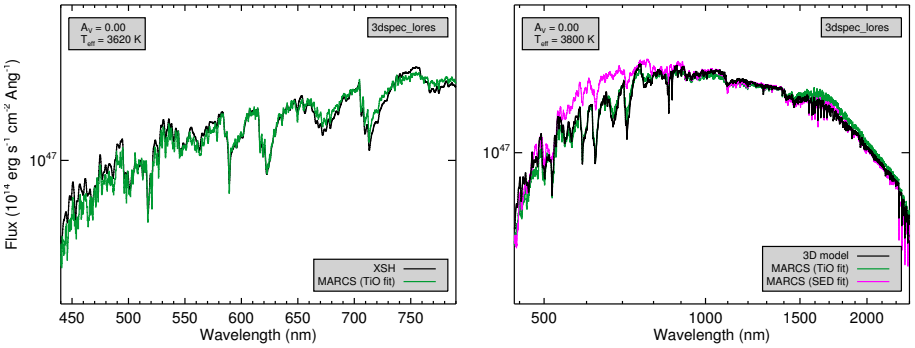

Fig. 7 A theoretical fit to the optical spectrum (left) and to the complete SED (right) for a red supergiant. 3D model atmospheres (black line) improve the consistency between the TiO bands and the IR 1.6μ diagnostics (Davies et al. 2013).

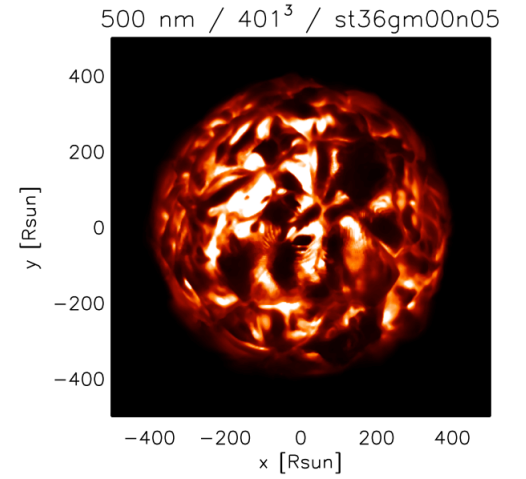

Fig. 8 Emergent intensity at 500 nm from a 3D RHD simulation of convection for a red supergiant Betelgeuse. The model is characterised by $T_{\rm eff} = 3710$ K, $\log g = 0.047$, and the solar metallicity. The cubic grid contains 401^3 nodes (Chiavassa et al, 2011).

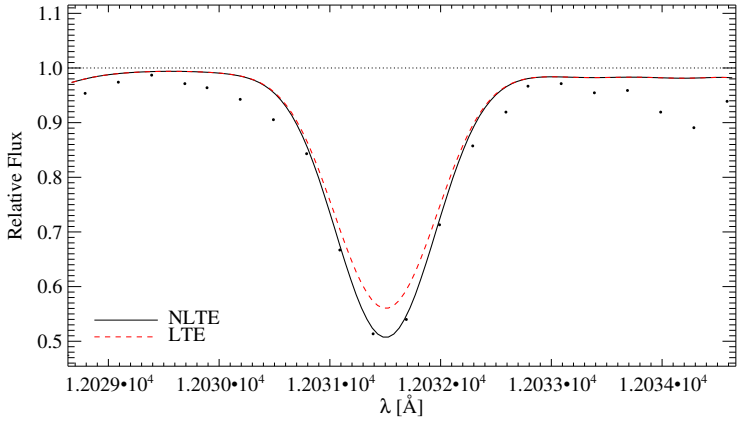

Fig. 9 Subaru/IRCS high resolution observations (black dots) J-band observations of Si I lines in the spectrum of the Per OB1 RSG HD 14270 (12031 $\AA$) compared with a LTE (red, dashed) and a NLTE (black, solid) fit. The fit profiles have been calculated with $T_{\rm eff} = 3800$ K, $\log g = 1.0$,$[Z] = 0.0$, and microturbulence $Vmic = 5$km/s (Bergemann et al, 2013).

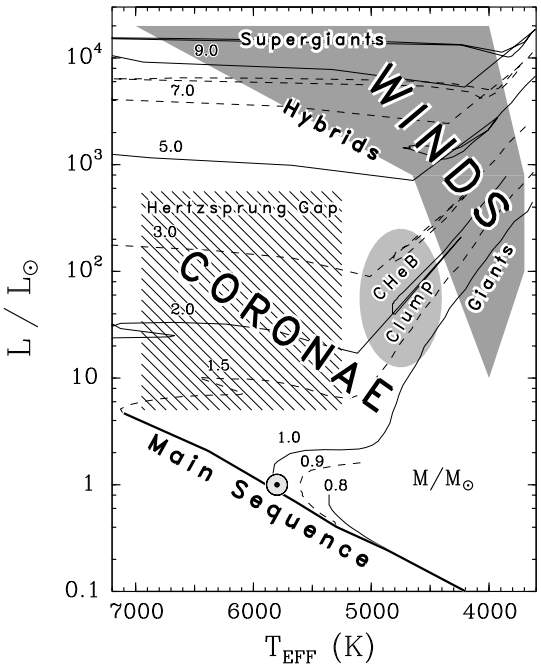

Fig. 10 An H-R diagram of late-type stars (Ayres, 2010). Stellar winds and chromospheres are typical for cool giants and supergiants.